Uniaxial pressure effects on spin-lattice coupled phase transitions in a geometrical frustrated magnet $CuFeO_2$

H. Tamatsukuri,* S. Aoki, S. Mitsuda, T. Nakajima,†
T. Nakamura, T. Itabashi, S. Hosaka, and S. Ito
Department of Physics, Faculty of Science,
Tokyo University of Science, Tokyo 162-8601, Japan

Y. Yamasaki† and H. Nakao
High Energy Accelerator Research Organization, Tsukuba, Ibaraki 305-0801, Japan

K. Prokes and K. Kiefer
Helmholtz-Centre Berlin for Materials and Energy,
Hahn-Meitner-Platz 1, Berlin 14109, Germany

(Dated: June 6, 2016)

Abstract

We have performed magnetic susceptibility, dielectric constant, neutron diffraction and synchrotron radiation x-ray diffraction measurements on a spin-lattice coupling system $CuFeO_2$ under applied uniaxial pressure p up to 600 MPa. We have found that the phase transition temperature T_{N1} from the paramagnetic phase to the partially disordered phase increases by as many as 5 K from original $T_{N1} \simeq 14$ K under applied p of 600 MPa and that a lattice constant b_m of $CuFeO_2$ remarkably changes. In contrast, the value of q_0, which is a magnetic modulation wave number at T_{N1} and should reflect ratios of the exchange coupling constants, is not changed even by applied p of 600 MPa. Based on these results, we show that the explanation using only the exchange striction effect is not suitable for the magnetic phase transition in $CuFeO_2$. These results suggest that a lattice degree of freedom via spin-lattice coupling is indispensable for determination of magnetic properties of $CuFeO_2$. Dielectric anomaly under applied p of 600 MPa is also briefly discussed.

PACS numbers: 75.30.Kz

I. INTRODUCTION

Geometrically spin frustrated systems provide fertile fields for modern condensed-matter physics research.[1] To lift the degeneracy in the vicinity of a grand state owing to the frustration, the systems tend to closely connect lattice degrees of freedom with spins. As a result, the spin-lattice couplings in the geometrically spin frustrated systems give rise to exotic magnetic phenomena, such as spin-Peierls transition,[2,3] spin-driven Jahn-Teller effect[4,5] and spin-driven ferroelectrics.[6]

Among the spin-lattice coupled systems, delafossite compound $CuFeO_2$ (CFO) is one of the vastly investigated material to understand the highly rich magnetic phase diagram including spin-driven ferroelectric phase.[7–20] CFO belongs to the $R\bar{3}m$ space group at room temperature ($a = b = 3.03$ Å, $c = 17.17$ Å in hexagonal notation). In CFO, Fe^{3+} ions ($S = 5/2$) form the triangular-lattice layers with antiferromagnetic interactions, which are stacked along the c axis. As shown in Fig. 1, with decreasing temperature (T) from a paramagnetic (PM) phase, the system enters a partially disordered (PD) phase with a magnetic modulation wave vector (q,q,3/2) [$q = 0.196$-0.220] at $T_{\rm N1} = 14$ K, in which the amplitude of spins along the c axis are sinusoidally modulated.[21,22] On further cooling to $T_{\rm N2} = 11$ K, a collinear 4-sublattice (4SL) phase (↑↑↓↓) with a magnetic modulation wave vector (1/4,1/4,3/2) is realized.[21,23]

These magnetic phase transitions are accompanied by a spontaneous lattice distortion from rhombohedral $R\bar{3}m$ to monoclinic $C2/m$.[9,11] In the lattice distortion, the monoclinic b axis ($b_{\rm m}$) elongates and the monoclinic a axis ($a_{\rm m}$) contracts, resulting in a deformation from the "equilateral" triangular-lattice in the PM phase to an "scalene" one in the 4SL phase, through a "isosceles" triangular-lattice in the PD phase,[10,19] as shown in Fig. 1. Hereafter, we add the subscript "m" to the monoclinic notations, and the [110] and the [1$\bar{1}$0] directions in hexagonal notation correspond to $[010]_{\rm m}$ and $[100]_{\rm m}$ directions in monoclinic notation, respectively (see Fig. 1). Several researchers have pointed out that the spin-lattice coupling in CFO systems plays a key role for the realization of the collinear ↑↑↓↓ magnetic structure as the ground state,[9,10] which is originally not expected by Heisenberg spin character of Fe^{3+} ion. This point is also consistent with theoretical work that the spin-lattice coupling stabilizes the collinear magnetic structures including the 4SL ↑↑↓↓ structure even in Heisenberg antiferromagnets.[24] Moreover, the nearest-neighbor exchange interaction

J_1 splits into three inequivalent interactions due to the the monoclinic lattice distortion. The split interactions successfully account for spin wave excitation in the 4SL phase[25] and ESR spectrum.[26]

As well as the investigations of the origin of the ground state and the value of the exchange constants at the low temperature, pressure effects for the magnetic properties of CFO have been investigated.[16–19] Because the lattice symmetry is broken by the spontaneous lattice distortion just at the phase transition temperature $T_{\rm N1}$, one expects that the application of pressure at this temperature provides a significant influence for the magnetic properties of CFO. Thus, we focus on an applied-pressure-impact on the exchange constants at $T_{\rm N1}$, hereafter, while pressure effects on the collinear 4SL magnetic structure at the low temperature should be fascinating objects. Although, in the vicinity of $T_{\rm N1}$, it is rather difficult to determine the exchange constants from spin waves, a magnetic modulation wave number "at phase transition temperature", q_0, is determined by a ratio of exchange constants in general, and thus, it should be a characteristic value.

Using neutron diffraction under an "isotropic" pressure up to 8 GPa, which suppresses the spontaneous lattice distortion, Terada *et al.* reported that the temperature variation of q in the PD phase is suppressed by the isotropic pressure, together with the rise of $T_{\rm N1}$.[17]

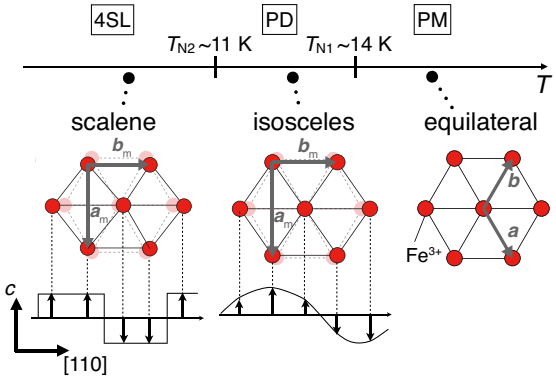

FIG. 1. (Color Online) Magnetic phase diagram of CFO as a function of temperature. Below $T_{\rm N2} \simeq 11$ K, a collinear 4-sublattice (4SL) phase ($\uparrow\uparrow\downarrow\downarrow$) with a magnetic modulation wave vector (1/4,1/4,3/2) is realized. In the range between $T_{\rm N2} \leq T \leq T_{\rm N1} \simeq 14$ K, a sinusoidal magnetic structure with a magnetic modulation wave vector $(q,q,3/2)$ [$q = 0.196$-0.220] is realized. Triangular lattices formed by Fe^{3+} ions in each phases are also schematically illustrated.

Besides, q_0 is varied from 0.195 (0 Pa) to ∼0.185 (5 GPa) (from 0.39 to 0.37 for q_{m0}) by the isotropic pressure, and finally at 8 GPa, short range order with temperature independent q remains at the lowest temperature.[16,17,27]

On the other hand, Nakajima *et al.* performed neutron diffraction, synchrotron x-ray diffraction and magnetic susceptibility measurements under an "anisotropic" uniaxial pressure up to 100 MPa along the $[1\bar{1}0]$ direction, which is conjugate direction to the spontaneous lattice distortion in CFO.[18,19] They observed the upward shift of $T_{\rm N1}$, which can be interpreted as a result of partial release of the spin frustration in this system by assistance of the spontaneous lattice distortion, and accompanied increment of structural transition temperature. Taking into account that uniaxial pressure, p, brakes the lattice symmetry, one can expect that a change in a ratio of the exchange constants by applied p is larger than those by the isotropic pressure, and that q_0, which should reflect the ratio of the exchange constants, also shows larger change. In previous study, however, pressure change in q_0 was not conclusive, and thus applied p up to 100 MPa is too small to investigate the p variation of q_0. Moreover, a p variation of lattice constant $b_{\rm m}$ is rather indistinguishable to discuss a change in the exchange constants determining q_0 through exchange striction effect.

Quite recently, we have developed a technique that allows the application of the uniaxial pressure p up to 600 MPa for CFO. In this paper, we report the results of magnetic susceptibility, dielectric constant, neutron diffraction and synchrotron radiation x-ray diffraction measurements on CFO under applied p up to 600 MPa. We have found that the value of q_0 is not changed even by applied p of 600 MPa despite a drastic rise of $T_{\rm N1}$. Moreover, the applied p of 600 MPa causes remarkable change in the $b_{\rm m}$ beyond the spontaneous lattice distortion, which should suggest a change in the exchange constants determining q_0 through exchange striction effect. Nevertheless, the exchange striction effect is not suitable for an explanation of these results. These results suggest that the lattice degree of freedom via spin-lattice coupling is indispensable for determination of magnetic properties in CFO.

II. EXPERIMENTAL DETAILS

Single crystals of CFO were prepared by the floating zone method.[28] The crystals were cut into dice-like shapes with typical dimensions of $1.36 \times 1.44 \times 1.70$ mm^3. The three axes of the dice-like samples are along [110], $[1\bar{1}0]$, and [001] directions and the sample was

mounted in a pressure cell used in ref. [18, 19, and 29] with the $[1\bar{1}0]$ axis vertical. The uniaxial pressure devices used in this work were also the same as used in these previous works: p along the vertical direction (therefore, $p \parallel [1\bar{1}0]$) is controlled by a SiCr coil spring and a micrometer attached on top of the cryostat, enabling us to control the magnitude of p even when the sample is at low temperatures, and p is monitored by a load meter. In all experiments in this study, p was always applied at 25 K. The temperature dependence of the magnetic susceptibility at the magnetic field of 100 Oe along the $[1\bar{1}0]$ direction were measured by a SQUID magnetometer (Quantum Design). The dielectric constant ϵ was measured at 10 kHz using an LCR meter (Agilent 4980A), where the electrodes were consisted of silver paste painted onto [110] surfaces.

Neutron-diffraction measurements under applied p were carried out at the two-axis diffractometer E4 installed at the Berlin Neutron Scattering Center in the Helmholtz Centre Berlin for Materials and Energy. The wavelength of incident neutron was 2.44 Å. The synchrotron radiation x-ray diffraction measurements under applied p was carried out at the beamline BL-3A in Photon Factory in High Energy Accelerator Research Organization, Tsukuba, Japan. The energy of the incident x-ray was tuned to 14 keV. Since the direction of p is parallel to the $[1\bar{1}0]$ direction, the scattering plane is the (H, H, L) plane in both of the diffraction measurements. Basically, we have performed these diffraction measurements in the same manner as in the previous experiments.[18,19]

III. RESULTS

Figure 2(a) shows a temperature dependence of magnetic susceptibility under ambient pressure and applied p of 600 MPa. At zero applied pressure, the T dependence of magnetic susceptibility is consistent with previous results.[18,30] With increasing p, $T_{\rm N1}$ drastically increases. The rise of $T_{\rm N1}$ under applied p of 600 MPa reaches 5 K from original $T_{\rm N1} \simeq 14$ K. The p dependence of $T_{\rm N1}$ are summarized in an inset of Fig. 2(a), which is linear extension of the previous result.[18] We have also found that the application of $p = 600$ MPa results in the upward shift of $T_{\rm N2}$ by ~ 1 K, whereas the upward shift of $T_{\rm N2}$ is only ~ 0.2 K up to 80 MPa.[18]

Figures 3(a)–3(d) show the typical neutron diffraction profiles on cooling under ambient pressure and applied p of 600 MPa. At 19.4 K, which is consistent with $T_{\rm N1}(p = 600{\rm MPa})$

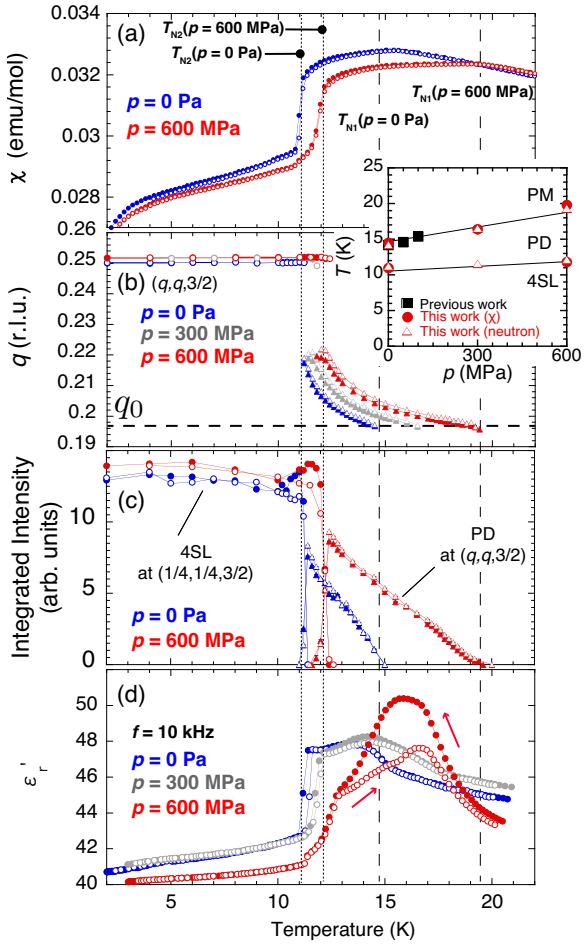

FIG. 2. (Color Online) Temperature dependence of (a) magnetic susceptibility χ, (b) magnetic modulation wave number q, (c) integrated intensity of the magnetic Bragg reflections, (d) (real part of) dielectric constant ϵ along the [110] axis, of CFO under the selected-applied p. Open and closed symbols denote the data for increasing and decreasing temperature processes, respectively. The figure extending over (a) and (b) shows a p - T phase diagram of CFO. The data indicated by black square symbols are redrawn from the data in Ref. 18.

obtained by the magnetic susceptibility, the magnetic reflection is observed at $(q,q,3/2)$, where $q \sim 0.196$ under applied p of 600 MPa. With decreasing T, the peak position shifts toward higher q value as shown in Fig. 3(a). These features correspond to the T dependence of the magnetic diffraction profiles in the PD phase under ambient pressure. Around 12 K under applied p of 600 MPa, the magnetic reflection at $(1/4,1/4,3/2)$ corresponding to the 4SL magnetic order coexists with the PD magnetic reflection, while they coexist at 11.2 K

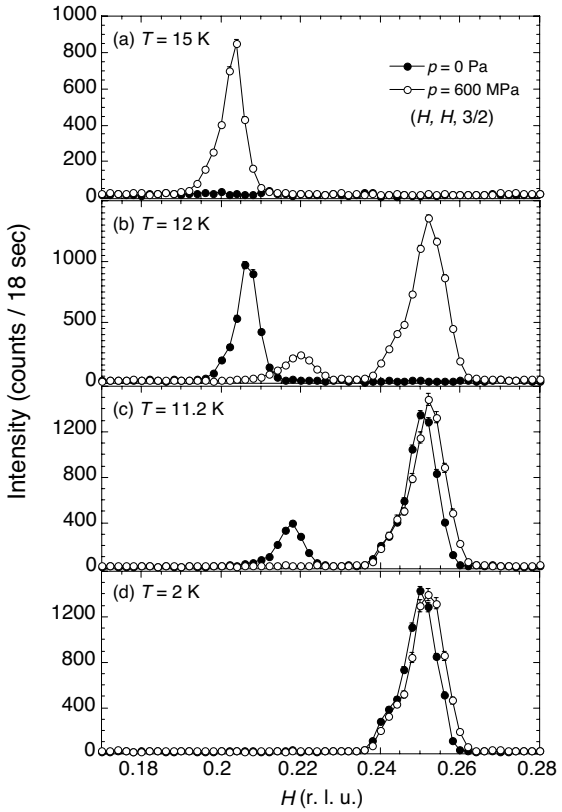

FIG. 3. (Color Online) Typical neutron diffraction profiles at (a) 15 K, (b) 12 K, (c) 11.2 K, (d) 2 K on cooling. The filled and open symbols denote the data measured under ambient pressure and applied p of 600 MPa, respectively.

at ambient pressure, as shown in Figs. 3(b) and 3(c). Finally below 11.8 K, the 4SL phase is realized under applied p of 600 MPa as shown in Fig. 3(d). The T dependence of q and the integrated intensity under selected applied p are summarized in Figs. 2(b) and 2(c). We did not observe any other magnetic reflections corresponding to an emergence of other magnetic ordering even under applied p of 600 MPa.

Here, we emphasize that the value of $q_0 \sim 0.196$, which is a magnetic modulation wave number at $T_{\rm N1}$, is almost not changed even by applied p of 600 MPa, as shown in Fig. 2(b), despite the drastic rise of $T_{\rm N1}$. Taking into account that q_0 should reflect ratio of the exchange constants, the p-independent q_0 would provide a strict condition for the p variation of the exchange constants due to the exchange striction effect. We will discuss this point later.

In order to investigate the lattice constants of CFO under $p = 600$ MPa, we have also per-

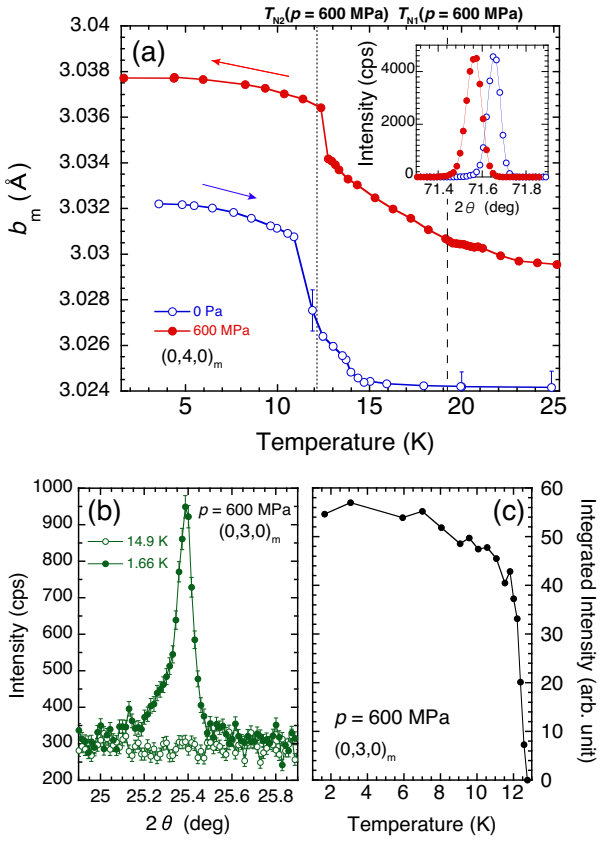

FIG. 4. (Color Online) (a) Temperature dependence of $b_{\rm m}$ under $p = 0$ and 600 MPa. Error bars of the $p = 600$ MPa data are within the size of the symbols. The data $p = 0$ are redrawn from Ref. 19. After we checked consistency in previous results from present-rough-mesh T dependence of $b_{\rm m}$, we have shifted the $p = 0$ data to modify a tiny difference of offset scattering angle, using the present reflection data ($p = 0$ MPa, $T = 25$ K) shown in an inset. Note that we show the T dependence of $b_{\rm m}$ under $p = 600$ MPa on cooling process, while that at ambient pressure in previous study was obtained on warming process.[19] We have observed, however, that there is no thermal hysteresis. (b) Typical x-ray profiles of the $(0, 3, 0)_{\rm m}$ superlattice reflection under $p = 600$ MPa at 14.9 K and 1.66 K. (c) Integrated intensity of the $(0, 3, 0)_{\rm m}$ superlattice reflection under p = 600 MPa as a function of temperature.

formed synchrotron radiation x-ray diffraction measurements similar to the previous study.[19] Figure 4(a) shows the temperature variations of $b_{\rm m}$ obtained by $(0, 4, 0)_{\rm m}$ reflections under p = 0 and 600 MPa. At $T_{\rm N1}(p = 600\ \text{MPa})$, which is determined by the magnetic susceptibility and neutron diffraction experiments, the structural transition is smeared by the application

of p, as was reported by T. Nakajima *et.al.*.[19] With further decreasing T under applied $p =$ 600 MPa, in contrast, $b_{\rm m}$ shows discontinuous jump near $T_{\rm N2}(p = 600$ MPa). Moreover, $b_{\rm m}$ under applied $p = 600$ MPa elongates from the equilateral $b_{\rm m}$ even at 25 K, at which the system is in the PM phase. The elongation of $b_{\rm m}$ at 25 K is almost comparable with those by the spontaneous lattice distortion at ambient pressure.

Figures 4(b) and 4(c) show typical diffraction profiles of the $(0, 3, 0)_{\rm m}$ superlattice reflections under $p = 600$ MPa, which arise from the correspondence to the scalene triangle distortion in the 4SL phase, and ther integrated intensity as a function of T, respectively. As shown in Fig. 4(c), the $(0, 3, 0)_{\rm m}$ superlattice reflection emerges at 12.8 K close to $T_{\rm N2}(p = 600$ MPa), even though $b_{\rm m}(T = 14$ K) ~ 3.033 Å under $p = 600$ MPa is larger than $b_{\rm m}(T = 4$ K) ~ 3.032 Å in the 4SL phase at zero applied pressure. This result indicates that the mere support of the only isosceles lattice distortion does not achieve the emergence of the 4SL magnetic ordering; the scalene triangle distortion is a key factor for the emergence of the 4SL magnetic ordering, as have been pointed out by several researchers.[9,10]

IV. DISCUSSION

Now, we consider an uniaxial pressure effect for the spin-lattice coupled phase transition in CFO. When p is applied, a displacement of magnetic ions should modify a spin Hamiltonian due to the exchange striction effect:[24,31,32]

$$\begin{aligned}\mathcal{H} &= \mathcal{H}_{\text{modified exchange}} + \mathcal{H}_{\text{lattice}}(\{\boldsymbol{u}_i\}) \\ &= J\sum_{<ij>}(1 - \alpha u_{ij})\boldsymbol{S}_i \cdot \boldsymbol{S}_j + \mathcal{H}_{\text{lattice}}(\{\boldsymbol{u}_i\}),\end{aligned} \tag{1}$$

where $\boldsymbol{u}_i$ is the displacement of site i, $u_{ij} = (\boldsymbol{u}_i - \boldsymbol{u}_j) \cdot \hat{\boldsymbol{e}}_{ij}$ is the relative change in length of the bond ij ($\hat{\boldsymbol{e}}_{ij}$ is the unit vector from site i to j), and $\alpha = J^{-1}\partial J/\partial r$ is the constant. In the spin-lattice coupled system, integrating $\mathcal{H}_{\text{mo. ex.}} + \mathcal{H}_{\text{lattice}}$ with $\boldsymbol{u}_i$ or u_{ij} generates an effective spin Hamiltonian including spin-lattice coupled term.[24,31,32] In the case of non spin-lattice coupled system, in contrast, $\mathcal{H}_{\text{lattice}}$ can be neglected even when exchange striction is affected by some external field at phase transition, and thus magnetic properties in the system (the phase transition temperature, a magnetic field or T dependence of magnetic modulation wave number and so on) can be explained by only the change in the exchange constants. For such an example, S. Kobayashi *et al.* quite recently reported that, in geometrically

frustrated but non spin-lattice coupled system $CoNb_2O_6$, q_0 in $CoNb_2O_6$ is easily modified by applied p.[33] Moreover, p variation of exchange constants estimated by p variation of q_0 are consistent with those estimated by p variation of phase transition fields, and thus, these results are well explained by the analysis using the mean-field approximation and only $\mathcal{H}_{\text{mo. ex.}}$ in $CoNb_2O_6$.[34]

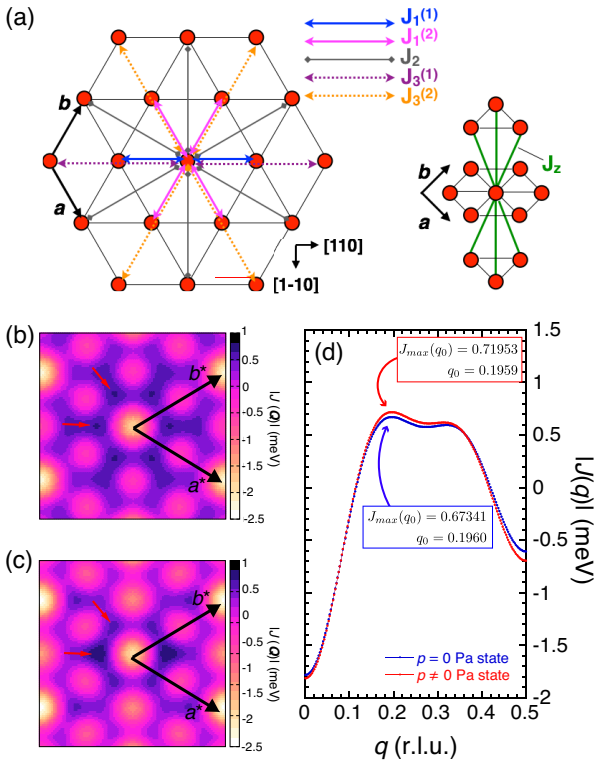

FIG. 5. (Color Online) (a) Paths of the exchange interactions. [(b)-(c)] $|J(\boldsymbol{Q})|$ contour map ($L = 3/2$) for (b) the $p = 0$ Pa state and (c) the (110) domain stabilized state by applied $p \parallel [1\bar{1}0]$, which is made by the exaggerated parameter sets for visibility. (d) q dependence of $|J(q)|$. "$p = 0$ Pa state" is drawn by the parameter sets $J_1^{(1)} = J_1^{(2)} = -0.147, J_2 = -0.05, J_3^{(1)} = J_3^{(2)} = -0.15, J_z = -0.05$, and "$p \neq 0$ Pa state" is drawn by the parameter sets $J_1^{(1)} = -0.140, J_1^{(2)} = -0.154, J_2 = -0.05, J_3^{(1)} = -0.159, J_3^{(2)} = -0.155, J_z = -0.05$.

In contrast, the discussion using only $\mathcal{H}_{\text{mo. ex.}}$ is not suitable for the case of CFO. Here, we show that the enhancement of T_{N1} is not explained by the exchange striction effect with only $\mathcal{H}_{\text{mo. ex.}}$ in the following. From our experiments, a temperature enhancement factor,

$\alpha_{\rm obs}$, is

$$\alpha_{\rm obs} \equiv \frac{T_{\rm N1}(p = 600\ {\rm MPa}) = 19\ {\rm K}}{T_{\rm N1}(p = 0\ {\rm Pa}) = 14\ {\rm K}} \simeq 1.36 \tag{2}$$

Within the mean-field approximation, the magnetic phase transition temperature $T_{\rm N1}$ is written by $3k_{\rm B}T_{N1} = S(S+1)|J_{\rm max}(\boldsymbol{Q}_0)|$ in general, where k_B is the Boltzmann constant, $S = 5/2$ for CFO, $\boldsymbol{Q} = H\boldsymbol{a}^* + K\boldsymbol{b}^* + L\boldsymbol{c}^*$ is the magnetic modulation vector, $|J_{\rm max}(\boldsymbol{Q}_0)|$ is a Fourier transformed maximum value of exchange constants and $\boldsymbol{Q}_0$ is $\boldsymbol{Q}$ providing the maximum value of $|J(\boldsymbol{Q})|$. Therefore,

$$\alpha_{\rm calc} \equiv \frac{|J^{p=600{\rm MPa}}_{\rm max}(\boldsymbol{Q}_0)|}{|J^{p=0{\rm Pa}}_{\rm max}(\boldsymbol{Q}_0)|} \tag{3}$$

should coincide with the temperature enhancement factor, as far as the exchange striction with only $\mathcal{H}_{\text{mo. ex.}}$ is concerned.

We define the exchange constants in CFO as those shown in Fig. 5(a)[35] for a (110) domain stabilization by the application of $p \parallel [1\bar{1}0]$, as described below in detail. Taking spin wave analysis by Nakajima *et al.* into consideration,[25,36] we have chosen the exchange constant values in meV unit as $J_1^{(1)} = J_1^{(2)}$ = -0.147, J_2 = -0.05, $J_3^{(1)} = J_3^{(2)}$ = -0.15 and J_z = -0.05 for the $p = 0$ Pa state. As expected the definition of the exchange constants, their Fourier transformation $J(\boldsymbol{Q})$ with these parameter values shows the six fold symmetry along the c axis as shown in Fig. 5(b).

Owing to the trigonal symmetry along the c axis, CFO has two other magnetic modulation vectors of (-2q,q,3/2) and (q,-2q,3/2), which are equivalent to $(q, q, 3/2)$. As a result, three magnetic domains exist. When we apply p to the sample along to the $[1\bar{1}0]$ direction, however, only the domain with $(q, q, 3/2)$ magnetic modulation vector, called (110) domain, is stabilized.[37,38] Therefore, we assume the single (110) domain state for the calculation of $|J_{\rm max}(\boldsymbol{Q}_0)|$, hereafter. When the (110) domain is stabilized, the peaks on the (110) axis grow and the other peaks shrink, as shown in Fig. 5(c) (see red arrows). Taking into account the experimental result that the magnetic diffraction peak in the (110) domain is on the (H,H,3/2) line, we can write $J(\boldsymbol{Q} = (q, q, 3/2))$ as $J(q)$:

$$\begin{aligned} J(q) = &-4J_1^{(1)}\cos(2\pi q) - 2J_1^{(2)}\cos(4\pi q) \\ &-2J_3^{(1)}\cos(4\pi q) - 2J_3^{(2)}\cos(8\pi q) \\ &-2J_2(\cos(6\pi q) + 1) + 2J_z(2\cos(2\pi q) + 1), \end{aligned} \tag{4}$$

Then, we obtain $|J_{\max}(\boldsymbol{Q}_0)| = |J_{\max}(q_0)|$, and q_0 is just the measurement value in our experiments. The parameter sets for the $p = 0$ Pa state described above provide $J(q)$ curve shown in Fig. 5(d) and consistently reproduce the experimental value $q_0 = 0.1960$.[39] $|J_{\max}^{p=0\mathrm{Pa}}(q_0)|$ is 0.673408.

Next, on the assumption that $p = 600$ MPa is applied along to the $[1\bar{1}0]$ direction, we prepared parameter sets by independently varying values of $J_1^{(1)}$, $J_1^{(2)}$, $J_3^{(1)}$ and $J_3^{(2)}$ within ± 5 %, which are considered to the most influencing parameters for $J(q)$ and q_0. Using these parameter sets, we calculated $J(q)$, q_0, and $|J_{\max}^{p\neq 0\mathrm{Pa}}(q_0)|$. Then, we surveyed parameter sets with consistency in the experimental result $0.1958 \leq q_0 \leq 0.1962$. In addition, we eliminated the parameter sets destabilizing (110) domain. For simplicity, J_2 and J_z were fixed.

We show one of calculation result in Fig. 5(d). This $J(q)$ curve is obtained by the parameter set providing the largest $|J_{\max}^{p\neq 0\mathrm{Pa}}(q_0)| = 0.71953$ (the value of parameters are shown in a caption of Fig. 5). As mentioned above, q_0 is determined by the ratio of the exchange constants. We can consider that a ratio of $J_3^{(2)}$ to $J_1^{(2)}$ is the most dominant for $J(q)$, because they are interactions in the [110] direction. Thus, we can assume by intuition that, if this interaction ratio is not changed under applied p, q_0 is also constant for applied p. Our calculation includes the parameter sets matching such naive scenario. However, α_{calc} is limited to 1.07 and does not explain α_{obs}, although obtained parameter sets may contain unphysical values. This means that the exchange striction effect using $\mathcal{H}_{\text{mo. ex.}}$ explains only about 20 % of α_{obs} at the most.

From our experimental results, b_{m} elongates by 0.2 % at 25 K. Taking into account the fractional change in the lattice parameters at ambient pressure reported by Terada *et al.*,[10] we assumed that a_{m} and c contract by 0.13 % and 0.06 %, respectively, at 25 K. Using these values, we roughly estimated a change in one of the Fe-O-Fe bond angles, and found that it is 0.05 %. Therefore, we conclude that the ± 5 % variation of J_1 and J_3 is relatively large, although there are no reason from the electronic bonding orbital theory. Nevertheless, α_{obs} is limited to 20 % at the most within the mean-field approximation and the exchange striction effect using only $\mathcal{H}_{\text{mo. ex.}}$. Thus, our results suggest that $\mathcal{H}_{\mathrm{lattice}}$ somehow contributes to even determination of T_{N1}.

Several specific expressions of $\mathcal{H}_{\mathrm{lattice}}$ have been proposed and biquadratic term generated by integration of $\mathcal{H}_{\text{mo. ex.}} + \mathcal{H}_{\mathrm{lattice}}$ plays important role for the realization of spin-lattice-coupled exotic state.[24,31,32] As for CFO, this biquadratic term reasonably explains

the existence of the collinear 4SL phase as the ground state. Besides the collinear magnetic structure of the ground state in CFO, several researches have pointed out the importance of the spin-lattice couplings for the phase transition even at T_{N1}. For example, Quirion *et al.* have suggested that the transition at T_{N1} is primary pseudoproper ferroelastic, with the spin acting as a secondary order parameter, from the ultrasonic velocity measurements and the analysis using Landau free energy.[11] Klobes *et al.* have also suggested that the magnetoelastic coupling persists in the PM phase as well, using nuclear resonance scattering.[20] Keeping these studies in mind, the magnetic properties of CFO such as $T_{\mathrm{N1,2}}$, q_0 or T dependence of q should also be treated by a theory including the appropriate spin-lattice coupling, in addition to the magnetic structures.

Finally, we show the temperature dependence of dielectric constant under applied p in Fig. 2(d). We have found that the temperature dependence of dielectric constant is drastically changed with large thermal hysteresis by applied p of 600 MPa. However, we have not observed the ferroelectric polarization and the T dependence of an imaginary part of dielectric constant remains 0 even under applied p of 600 MPa. Recently, N. Terada *et al.* reported that spiral magnetic ordering with ferroelectricity is induced by isotropic pressure $\sim$ 3 GPa.[17] Taking into account this report, one possible explanation of this anomalous dielectric property is that the drastic change in T dependence of ϵ may reflect the precursor of emergence of spiral magnetic ordering with ferroelectricity. The application of larger magnitude of p may be a promising way to investigate the spin-lattice coupled multiferroic phase.

V. CONCLUSIONS

In conclusion, we have found that the value of q_0 in $CuFeO_2$ is not changed even by applied p of 600 MPa despite a drastic rise of T_{N1}, using magnetic susceptibility, neutron diffraction and synchrotron radiation x-ray diffraction measurements under applied uniaxial pressure up to 600 MPa. This result suggests that, in addition to the magnetic structures, magnetic properties such as magnetic phase transition temperature, magnetic modulation wave number at phase transition and its T dependence should be treated by a theory including the appropriate spin-lattice coupling. Moreover, we have found that he temperature dependence of dielectric constant is drastically changed with large thermal hysteresis by applied p of 600

MPa. To investigate this dielectric anomaly, the application of larger magnitude of p would be helpful.

ACKNOWLEDGMENTS

We thank HZB for the allocation of neutron beamtime. The neutron diffraction experiments at HZB was carried out according to Proposal No. PHY-01-3177, which was transferred from HQR(T1-1) installed at JRR-3 with the approval of Institute for Solid State Physics, The University of Tokyo (proposal no. 12658), Japan Atomic Energy Agency, Tokai, Japan. This study has been approved by the Photon Factory Program Advisory Committee (Proposal No. 2013G676). This work was supported by a Grant-in-Aid for Scientific Research (C) (Grant Nos. 23540424 and 26400369) from Japan Society for the Promotion of Science.

---

* E-mail address: tamatsukuri@nsmsmac4.ph.kagu.tus.ac.jp

† Present address: RIKEN Center for Emergent Matter Science (CEMS), Saitama 351-0198, Japan

[1] R. Moessner and A. P. Ramirez, Phys. Today **59**, 24 (2006).

[2] F. Becca and F. Mila, Phys. Rev. Lett. **89**, 037204 (2002).

[3] K. Kodama, M. Takigawa, M. Horvatic, C. Berthier, H. Kageyama, Y. Ueda, S. Miyahara, F. Becca, and F. Mila, Science **298**, 395 (2002).

[4] Y. Yamashita and K. Ueda, Phys. Rev. Lett. **85**, 4960 (2000).

[5] O. Tchernyshyov, R. Moessner, and S. L. Sondhi, Phys. Rev. Lett. **88**, 067203 (2002).

[6] Y. Tokura, S. Seki, and N. Nagaosa, Rep. Prog. Phys. **77**, 076501 (2014).

[7] T. Kimura, J. C. Lashley, and A. P. Ramirez, Phys. Rev. B **73**, 220401(R) (2006).

[8] T. Nakajima, S. Mitsuda, S. Kanetsuki, K. Tanaka, K. Fujii, N. Terada, M. Soda, M. Matsuura, and K. Hirota, Phys. Rev. B **77**, 052401 (2008).

[9] F. Ye, Y. Ren, Q. Huang, J. A. Fernandez-Baca, P. Dai, J. W. Lynn, and T. Kimura, Phs. Rev. B **73**, 220404(R) (2006).

[10] N. Terada, S. Mitsuda, H. Ohsumi, and K. Tajima, J. Phys. Soc. Jpn. **75**, 023602 (2006).

[11] G. Quirion, M. J. Tagore, M. L. Plumer, and O. A. Petrenko, Phys. Rev. B **77**, 094111 (2008).

[12] G. Quirion, M. L. Plumer, O. A. Petrenko, G. Balakrishnan, and C. Proust, Phys. Rev. B **80**, 064420 (2009).

[13] M. L. Plumer, Phys. Rev. B **78**, 094402 (2008).

[14] T. T. A. Lummen, C. Strohm, H. Rakoto, and P. H. M. van Loosdrecht, Phys. Rev. B **81**, 224420 (2010).

[15] N. Terada, S. Mitsuda, Y. Tanaka, Y. Tabata, K. Katsumata, and A. Kikkawa, J. Phys. Soc. Jpn. **77**, 054701 (2008).

[16] N. Terada, T. Osakabe, and H. Kitazawa, Phys. Rev. B **83**, 020403 (2011).

[17] N. Terada, D. D. Khalyavin, P. Manuel, T. Osakabe, P. G. Radaelli, and H. Kitazawa, Phys. Rev. B **89**, 220403 (2014).

[18] T. Nakajima, S. Mitsuda, K. Takahashi, K. Yoshitomi, K. Masuda, C. Kaneko, Y. Honma, S. Kobayashi, H. Kitazawa, M. Kosaka, N. Aso, Y. Uwatoko, N. Terada, S. Wakimoto, M. Takeda, and K. Kakurai, J. Phys. Soc. Jpn. **81**, 094710 (2012).

[19] T. Nakajima, Y. Iguchi, H. Tamatsukuri, S. Mitsuda, Y. Yamasaki, H. Nakao, and N. Terada, J. Phys. Soc. Jpn. **82**, 114711 (2013).

[20] B. Klobes, M. Herlitschke, K. Z. Rushchanskii, H.-C. Wille, T. T. A. Lummen, P. H. M. van Loosdrecht, A. A. Nugroho, and R. P. Hermann, Phys. Rev. B **92**, 014304 (2015).

[21] S. Mitsuda, N. Kasahara, T. Uno, and M. Mase, J. Phys. Soc. Jpn. **67**, 4026 (1998).

[22] In Ref. 20, Krobes *et al*. have suggested that the magnetic structure in the range between $T_{\mathrm{N2}} \leq T \leq T_{\mathrm{N1}}$ is incompatible with the sinusoidal one. This suggestion, however, does not disturb our results and discussion, because our discussion is independent of specific magnetic structures.

[23] M. Mekata, N. Yaguchi, T. Takagi, T. Sugino, S. Mitsuda, H. Yoshizawa, N. Hosoito, and T. Shinjo, J. Phys. Soc. Jpn. **62**, 4474 (1993).

[24] F. Wang and A. Vishwanath, Phys. Rev. Lett. **100**, 077201 (2008).

[25] T. Nakajima, A. Suno, S. Mitsuda, N. Terada, S. Kimura, K. Kaneko, and H. Yamauchi, Phys. Rev. B **84**, 184401 (2011).

[26] S. Kimura, T. Fujita, N. Nishihagi, H. Yamaguchi, T. Kashiwagi, M. Hagiwara, N. Terada, Y. Sawai, and K. Kindo, Phys. Rev. B **84**, 104449 (2011).

[27] Although q_0 is reported to be ~ 0.192 in Ref. 16, the fact remains that temperature variation is locked and finally short range order with q_0 is realized.

[28] T. R. Zhao, M. Hasegawa, and H. Takei, J. Cryst. Growth **166**, 408 (1996).

[29] T. Nakajima, S. Mitsuda, T. Nakamura, H. Ishii, T. Haku, Y. Honma, M. Kosaka, N. Aso, and Y. Uwatoko, Phys. Rev. B **83**, 220101 (2011).

[30] The value of $T_{\rm N1} \sim 15.3$ K is relatively high (usually $T_{\rm N1} \simeq 14$ K in some literatures[9]). This may be accidentally caused by effective application of p for the sample because of experimental setup condition.

[31] K. Penc, N. Shannon, and H. Shiba, Phys. Rev. Lett. **93**, 197203 (2004).

[32] D. L. Bergman, R. Shindou, G. A. Fiete, and L. Balents, Phys. Rev. B **74**, 134409 (2006).

[33] S. Kobayashi, S. Hosaka, H. Tamatsukuri, T. Nakajima, S. Mitsuda, K. Prokeš, and K. Kiefer, Phys. Rev. B **90**, 060412 (2014).

[34] S. Mitsuda, unpublished.

[35] Note that the definition of $J_1^{(1)}$ and $J_1^{(2)}$ is different from used one in Refs. 25, 36, and 40. In the spin waves analysis in these papers, Nakajima *et al.* defined $J_1^{(1)}$ and $J_1^{(2)}$ base on the magnetostriction effect including the displacement of O^{2-} ions. On the other hand, we discuss the magnetic phase transition at $T_{\rm N1}$, and thus we consider only the exchange striction effect based on the relative change in the lattice distance, instead of the magnetostriction effect depending on the magnetic structure.

[36] T. Nakajima, N. Terada, S. Mitsuda, and R. Bewley, Phys. Rev. B **88**, 134414 (2013).

[37] S. Mitsuda, K. Yoshitomi, T. Nakajima, C. Kaneko, H. Yamazaki, M. Kosaka, N. Aso, Y. Uwatoko, Y. Noda, M. Matsuura, N. Terada, S. Wakimoto, M. Takeda, and K. Kakurai, J. Phys.: Conf. Ser. **340**, 012062 (2012).

[38] T. Nakajima, S. Mitsuda, T. Haku, K. Shibata, K. Yoshitomi, Y. Noda, N. Aso, Y. Uwatoko, and N. Terada, J. Phys. Soc. Jpn. **80**, 014714 (2011).

[39] Although the values of these parameters reproduce q_0 value, they are slightly different from them in Refs. 25, 36, and 40. Taking into account that the exchange parameters in the low temperature should differ from them at $T_{\rm N1}$, we believe that this slight difference would be appropriate.

[40] T. Nakajima, S. Mitsuda, J. T. Haraldsen, R. S. Fishman, T. Hong, N. Terada, and Y. Uwatoko, Phys. Rev. B **85**, 144405 (2012).